Tropical Journal of Pharmaceutical Research August 2024; 23 (8): 1239-1247
ISSN: 1596-5996 (print); 1596-9827 (electronic)

Available online at http://www.tjpr.org
http://dx.doi.org/10.4314/tjpr.v23i8.2

Original Research Article

Ginsenoside R3 alleviates non-alcoholic fatty liver disease by regulating the PPARγ/miR-103-3p pathway

Chenyi Li, Danjun Fan*
Department of Medical Care for Cadres, Zhejiang Hospital, No. 12 Lingyin Road, Hangzhou, Zhejiang 310012, China

For correspondence:* ***Email:* *fandj2007@sina.com;* ***Tel:*** *+86-13357106890*

Sent for review: 21 December 2023 *Revised accepted: 28 July 2024*

Abstract

Purpose: *To determine the effect of ginsenoside R3 (Rg3) on non-alcoholic fatty liver disease (NAFLD), and the mechanism involved.*
Methods: *High-fat diet (HFD) was used to establish an NAFLD mouse model. The mice were daily and intraperitoneally injected with Rg3 at a dose of 1 mg/kg. Blood lipid levels and levels of liver inflammatory markers were measured by enzyme-linked immunosorbent assay (ELISA) while liver pathological changes and lipid accumulation were assessed with hematoxylin-eosin (H&E) staining and oil red O staining, respectively. The mRNA and protein expressions of miR-103-3p and PPARγ were determined with quantitative real-time polymerase chain reaction (qPCR) and western blot assay, respectively. Furthermore, an in vitro hepatocyte NAFLD model was established, and Rg3 was used to treat the cells; PPARγ was overexpressed in the cells. Lipid accumulation, inflammatory factors, as well as PPARγ and miR-103-3p expressions were assessed as indicated for the in vivo studies above. Apoptosis was determined by flow cytometry.*
Results: *Rg3 alleviated the NAFLD-induced decreases in liver function, reversed NAFLD-mediated pathological injury in liver tissue injury, and decreased hepatic lipid build-up and inflammatory lesions ($p < 0.05$). It also significantly reversed the upregulation of PPARγ and miR-103-3p in the liver tissue of NAFLD mice. At the cellular level, Rg3 significantly inhibited free fatty acid (FFA)-induced lipid accumulation, apoptosis and inflammatory factors in primary mouse hepatocytes. The PPARγ overexpression counteracted the inhibitory effect of Rg3 on hepatocyte apoptosis, and increased miR-103-3p expression ($p < 0.05$).*
Conclusion: *These data suggest that Rg3 mitigates NAFLD through regulation of the PPARγ/miR-103-3p pathway. Therefore, Rg3 may be suitable for the treatment of NAFLD. However, clinical trials are required to ascertain the validity of this therapeutic strategy in clinical practice.*

Keywords: *Non-alcoholic fatty liver disease (NAFLD), Ginsenoside R3, PPARγ, miR-103-3p*

Tropical Journal of Pharmaceutical Research is indexed by Science Citation Index (SciSearch), Scopus, Web of Science, Chemical Abstracts, Embase, Index Copernicus, EBSCO, African Index Medicus, JournalSeek, Journal Citation Reports/Science Edition, Directory of Open Access Journals (DOAJ), African Journal Online, Bioline International, Open-J-Gate and Pharmacy Abstracts

INTRODUCTION

Non-alcoholic fatty liver disease (NAFLD) is a pathological condition characterized by the accumulation of fat in the liver and the degeneration of liver fat as a result of alcohol and other liver-damaging factors. The prevalence of NAFLD has steadily been on the rise, and it has gradually become the most prevalent liver disease affecting humans globally [1]. The pathogenesis of NAFLD is complex. Currently,

the ‘Second strike’ theory is widely acknowledged. The theory posits that insulin resistance causes lipid deposition in hepatocytes, representing the first hit of the disease which subsequently leads to impaired mitochondrial function, ER stress and oxidative damage, thereby causing liver lesions [2].

Insulin sensitizers, lipid-regulating drugs, hepatoprotective and enzyme-lowering drugs, and antioxidants are typical drugs used for the treatment of NAFLD [3]. These drugs may produce varying degrees of improvements in liver enzyme activities or glycolipid metabolism. However, most of them are not particularly effective in reducing liver inflammation, and the drugs often cause numerous adverse reactions [4]. Moreover, a discontinuation of their use may result in disease rebound [5]. As a result, the effective prevention and treatment of NAFLD remains a clinical challenge. Therefore, it is important to explore alternative and more effective intervention measures.

Several bioactive components derived from traditional Chinese medicine have demonstrated superior effectiveness in the treatment of NAFLD, with minimal adverse reactions, when compared to conventional Western medicine [6]. For example, *Chaihu* saponins alleviate liver damage induced in mice by thioacetamide and NAFLD through inhibition of inflammatory reactions and by acting as antioxidants [7]. *Schisandra chinensis* B enhances fatty acid oxidation by inhibiting liver steatosis and activating autophagy via the AMPK/mTOR pathway [8].

Ginsenoside R3 (Rg3) is a major component of red ginseng, and it accounts for a significant portion of the pharmacological effects of red ginseng such as immune regulation, as well as anticancer and antioxidant activities. Besides, Rg3 has been studied for its potential to ameliorate liver steatosis due to fat-rich diet [9]. However, the effect of Rg3 on repair of NAFLD-induced liver damage is yet to be studied.

Based on their structures and functions, peroxisome proliferator-activated receptors (PPARs) may be classified into three subtypes: PPARα, PPARδ (β) and PPARγ. Synthetic PPARγ ligands have been used to treat diabetes [10]. A specific example of these ligands is thiazolidinedione. On the other hand, PPARγ antagonists promote the uptake and storage of free fatty acids in adipose tissue while inhibiting the synthesis of fats found in adipose tissue. These antagonists exhibit anti-inflammatory effects and effectively improve insulin resistance [11]. In recent years, it has been found that rosiglitazone (RGZ) activates PPARγ, leading to increased fat synthesis and accelerated obesity [12].

In recent years, the relationship between miRNA and various liver illnesses has gained increasing consideration. Already, miRNA has been found to be widely present in the liver where it plays significant roles in pathogenesis of various hepatic ailments, e.g., NAFLD, with potential implications for disease severity. A study showed that PPARγ affects the adipogenesis process in mice by controlling miR-103-3p [11]. Additionally, miR-103-3p has been found to enhance liver steatosis and exacerbate NAFLD by targeting ACOX1 [13].

However, the mitigating effect of miRNA-103 on NAFLD-induced liver cell damage, and the associated mechanism, require further investigation. This was the major objective of this study.

EXPERIMENTAL

Animal studies

Twenty-four male C57BL/6J mice (age: 4 - 6 weeks) on a seven-day adaptive feeding period were randomly assigned to three groups of eight mice each. Eight mice (normal control) received *par* diet, while the remaining 16 mice were fed on HFD (about 1.67 kcal/g), comprising 79.5 % corn meal, 0.5 % cholesterol and 20 % lard. Four weeks later, 8 mice in the HFD group were intraperitoneally injected with Rg3 (1 mg/kg) daily (HFD +RG3 group), while the remaining 8 mice (HFD mice) received equivalent amount of physiological saline, in place of Rg3. After 8 weeks, all the mice were euthanized, and the wet weights of the liver and body weights of mice were obtained.

The liver tissues were preserved using two different methods, with one half fixed in 40 g/L paraformaldehyde solution, while the other half was freeze-dried in liquid nitrogen tanks and then transferred to -80 ℃ prior to use.

Ethical matters

The mice were obtained from Hangzhou Medical College Laboratory Animal Center. The research protocol received approval from the ethical authority of Institutional Animal Care and Use Committee, Zhejiang Center of Laboratory Animals (approval no.: ZJCLA-IACUC-20050085), and followed international guidelines for animal studies.

Cell culture and treatment

After anesthesia, the mice were intubated through the portal vein, and the inferior vena cava was cut off. The liver was flushed with DMEM so as to remove blood, and then digested with collagenase II for 10 min. The mouse primary hepatocytes (MPHs) suspension was isolated. After a 5-min centrifugation in the cold at 100 g, cell suspension was made in 5 % PBS. The suspension of cells was then evenly distributed into 6 wells in a 37 ℃, 5 % CO_2 incubator. The medium was replaced after the primary liver cells adhered to the wall. The primary liver cells were incubated with FFA, a mixture of oleic acid (OA, Sigma Aldrich, St Louis, USA) and palmitic acid (PA, Sigma Aldrich, St. Louis, USA) at a ratio of 3:1. After incubating the MPHs with FFA for 48 h, the MPHs were harvested and used to establish an *in vitro* cell model. Simultaneously, cells in the model group were treated with 50 μM Rg3.

Cell transfection

Based on the kit manufacturer's instruction manual, transfection was done using 2 μg of pcDNA-PPARγ (GenePharma, Shanghai, China) and 3:1 mixture of 2 μg of pcDNA in Lipofectamine 2000 (Thermo Fisher Scientific, Waltham, MA, USA). The culture medium was changed after 4 h of cell transfection.

Hematoxylin-eosin (H&E) staining

Mouse liver tissue was fixed in 4 % paraformaldehyde for 72 h, and subjected to conventional H&E staining. After undergoing gradient dehydration and clearing, the liver tissue was embedded in paraffin and sliced. Then, the sections were de-paraffinized, re-hydrated in alcohol gradient, and subjected to hematoxylin staining, followed by differentiation using 70 % hydrochloric acid ethanol. Eosin staining was then performed, followed by dehydration and xylene-based clearing. After sealing using neutral gum, the liver tissue morphology was examined under a Leica light microscope (model no. M125 C).

Oil red O staining

In liver tissue studies, 10-μm frozen liver tissue sections were taken and subjected to 4 % paraformaldehyde fixation for ½ h. Then, the sections were subjected to 10-min staining with 0.5 % Oil Red O solution in isopropanol which was diluted with H_2O (3:2 ratio) before use (after filtration). On sealing with 80 % glycerol, the degree of lipid buildup in the liver tissue stained with Oil Red O was examined and photographed under a microscope. For cell studies, paraformaldehyde-fixed cells were stained with Oil Red O dye for 10 min. Following sealing with 80 % glycerol, the lipid accumulation in the cells fixed with Oil Red O was examined and photographed using a Leica light microscope (M125 C).

Enzyme-linked immunosorbent assay (ELISA)

On completion of the treatments, the mice were fasted overnight. Blood samples were collected by removing the eyeballs under anesthesia. The blood specimens were allowed to stand for 30 min and centrifuged at 3000 rpm for 10 min at 4 ℃. The supernatants (sera) were subjected to assays of serum levels of HDL-C, AST, LDL-C, ALT, triglycerides (TGs) and total cholesterol (TC), using kits in line with the kit manufacturers' instructions provided in the kit manuals. All the test kits used were provided by Nanjing Jiancheng Bioengineering Institute, China.

Flow cytometry

The MPHs were seeded into 24-well plates at a density of 1×10^7 cells/well and grown for 2 days. Thereafter, the cells in each well were trypsin-digested without the addition of EDTA, and then centrifuged at 2000 rpm for 5 min. Next, the cells were rinsed 3 times with PBS and re-suspended in 400 μL of the binding buffer, followed by incubation for 20 min at 4 ℃ in the dark after adding 5μL of AnnexinV-FITC (KeyGEN BioTECH, Jiangsu, China). Cell apoptosis rate was determined using a BD LSRFortessa™ X-20 flow cytometer (BD Biosciences).

qRT-PCR

TRIzol kits were employed for extraction of total RNA in line with the manufacturer's instructions. A 20-microlitre reaction system was used in the real-time PCR with SYBR Green Premix Ex Taq (Thermo Fisher Scientific, Waltham, MA, USA) on Light Cycler480 (Roche, Hvidovre, Denmark). For miRNA detection, the miScript II RT kit from Thermo Fisher Scientific was used to reverse-transcribe the total RNA to cDNA. The mRNA expression levels were determined by normalization to U6, the internal invariant control. Table 1 shows the primer sequences used. The cycling conditions were: 95 ℃ for 10 min, followed by 40 cycles, with each cycle denaturing at 95 ℃ for 15 sec, annealing at 60 ℃ for 1 min, and extending at 72 ℃ for 1 min. The relative

mRNA expression levels were calculated based on the $2^{-\Delta\Delta Ct}$ method.

Western blot assay

Freeze-dried liver tissue was fully ground and subjected to protein extraction using cold RIPA lysis buffer. The lysate was centrifuged at 4 ℃ and 13000 g for 10 min, and the protein concentration of the supernatant was determined. An appropriate amount of protein was mixed thoroughly with SDS-PAGE sampling buffer and denatured at 100 ℃ for 5 min. The sample volume of each group was calculated based on a loading amount of 60 µg. After SDS-PAGE, the sample was put onto a PVDF membrane at constant pressure and the membrane was incubated with 5 % skim milk for 60 min, followed by 12 h incubation at 4°C with specific antibody PPARγ and GAPDH (1:1000 dilution). Thereafter, the membrane was washed 3 times with PBS, followed by incubation with goat anti-rabbit IgG (# 14708, 1:1000, CST) at room temperature for 1 h. After another round of membrane washing, ECL chemiluminescence staining was performed. The grayscale value was analyzed, and the expression prototype of the target protein was determined by calculating the ratio of the target protein to the reference protein in the system.

Statistical analysis

The SPSS 22.0 software was used for statistical analysis. The data are presented as mean ± SD. Multi-group comparison was done with ANOVA, while two-group comparison was performed with *t*-test. Values of $p < 0.05$ were considered significant.

RESULTS

Influence of Rg3 on body and liver weights, and serum biochemical indicators in NAFLD mice

The results shown in Figure 1 reveal that mice in HFD group exhibited significantly greater body and liver weights than mice in the control group. There were increased blood levels of TG, AST, LDL-C, TC and ALT, while HDL-C levels were decreased. When compared to HFD group, Rg3 treatment reduced body and liver weights, lowered the serum concentrations of ALT, AST, LDL-C, TG and TC, and raised HDL-C levels (Figure 1 A - H). These results indicate that Rg3 alleviated damage to liver function in NAFLD mice.

Effect of Rg3 on liver injury, lipid accumulation and inflammation in NAFLD mice

The control group of mice exhibited normal liver lobular structure with round and centered nuclei, clear hepatic cords, and non-narrow hepatic sinuses. No cytoplasmic orange-red fat droplets were observed. On the other hand, the HFD mice showed liver cell swelling and degeneration of liver cells, with significant increases in the volume and number of lipid droplets and vacuoles in the cytoplasm.

Table 1: Primer pairs employed in PCR

Variable	Forward	Reverse
miR-103-3p	5 '- ACACTCCAGCTGGGAGCAGCATTGTAC-3'	5'-TGGTGTCGTGGAGTCG-3'
U6	5 '- CTCGTTCGAGACACA-3'	5 '- ACAGCTTCACGATTTGGT-3'

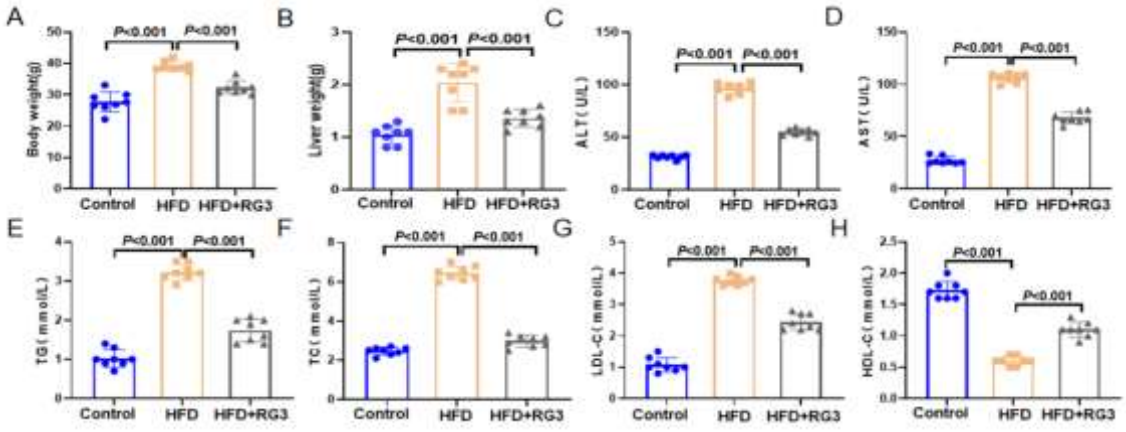

Figure 1: Effect of RG3 treatment on mouse parameters. (A) Mouse body weight; (B) Mouse liver weight; (C – H) Serum levels of ALT, AST, TG, TC, LDL-C, HDL-C

However, in the HFD group, the mice treated with Rg3 had reduced lipid droplet formation, restored liver cell volume, and alleviated hepatic sinus stenosis (Figure 2 A and B).

The HFD group showed higher levels of inflammatory factors than control cohort. However, Rg3 treatment lowered the levels of these inflammatory factors, and also significantly alleviated liver injury, lipid accumulation and inflammation in the mice (p<0.05; Figure 2 C – E).

Effect of Rg3 on PPARγ and miR-103-3p in the liver tissue of NAFLD mice

The results showed that PPARγ and miR-103-3p expressions in the HFD group were more up-regulated than in control mice. However, in HFD group, Rg3 treatment significantly decreased the expressions of PPARγ and miR-103-3p (Figure 3 A and B).

Effect of Rg3 on MPH

Lipid build-up in the OA + PA MPH was significantly greater than that in the control group (p < 0.05). In contrast, Rg3 alleviated lipid accumulation in MPH (Figure 4 A). In OA+PA MPH, there was significantly higher level of apoptosis than in the control MPH, while Rg3 inhibited MPH apoptosis (Figure 4 B). Moreover, OA+PA up-regulated TNF-α, IL-6 and IL-1β, but Rg3 reversed this trend by decreasing levels of IL-6, IL-1β, TNF-α and other inflammatory factors (Figure 4 C – E). Relative to the control group, PPARγ and miR-103-3p were up-regulated in OA+PA MPH but their expressions were inhibited by Rg3 (Figure 4 F and G). These data suggest that Rg3 suppressed liver cell damage and reduced the accumulation of lipids and inflammation in liver cells. This effect was most likely achieved through regulation of the expressions of PPARγ and miR-103-3p.

Rg3 alleviated hepatocyte injury via miR-103-3p by regulating PPARγ

The *in vitro* studies using hepatocytes was intended to provide insight into the mechanism through which Rg3 regulated PPARγ/miR-103-3p pathway. The results obtained indicate that the expression of PPARγ in MPH after overexpression of PPARγ was significantly up-regulated (p < 0.05). Overexpression of PPARγ reduced the inhibition of Rg3-induced MPH apoptosis. Moreover, Rg3 inhibited the expression of miR-103-3p in MPH, and the expression of miR-103-3p was up-regulated after overexpression of PPARγ (p < 0.05; Figure 5 A and C). Thus, Rg3 Inhibited liver cell injury by regulating miR-103-3p expression via PPARγ.

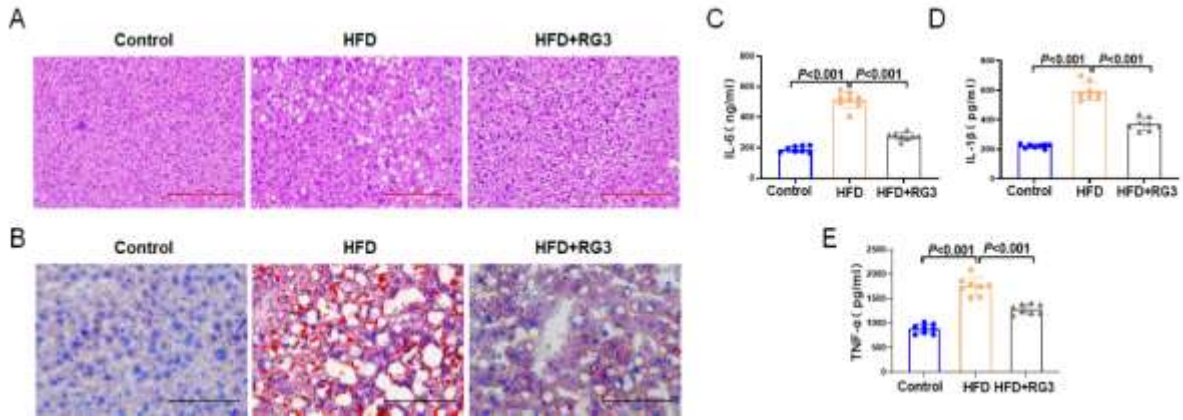

Figure 2: (A) Abnormal mutations in mouse liver tissue spotted via H & E staining. (B) Lipid buildup in mouse liver tissue seen via oil red O staining. (C – E) Concentrations of inflammatory factors in mouse liver tissue

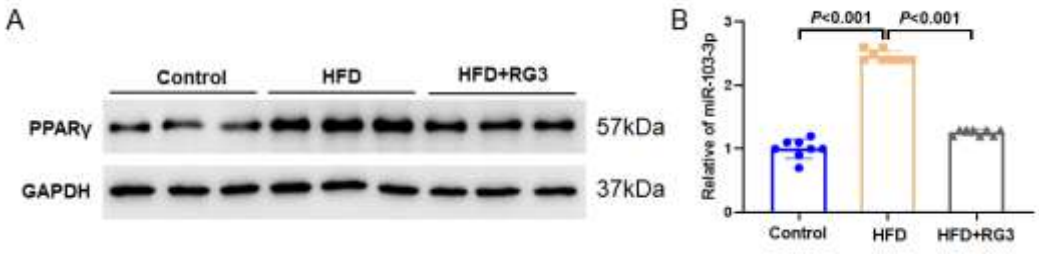

Figure 3: (A) PPARγ expressions in mouse liver tissue; (B) miR-103-3p expressions in mouse liver tissue

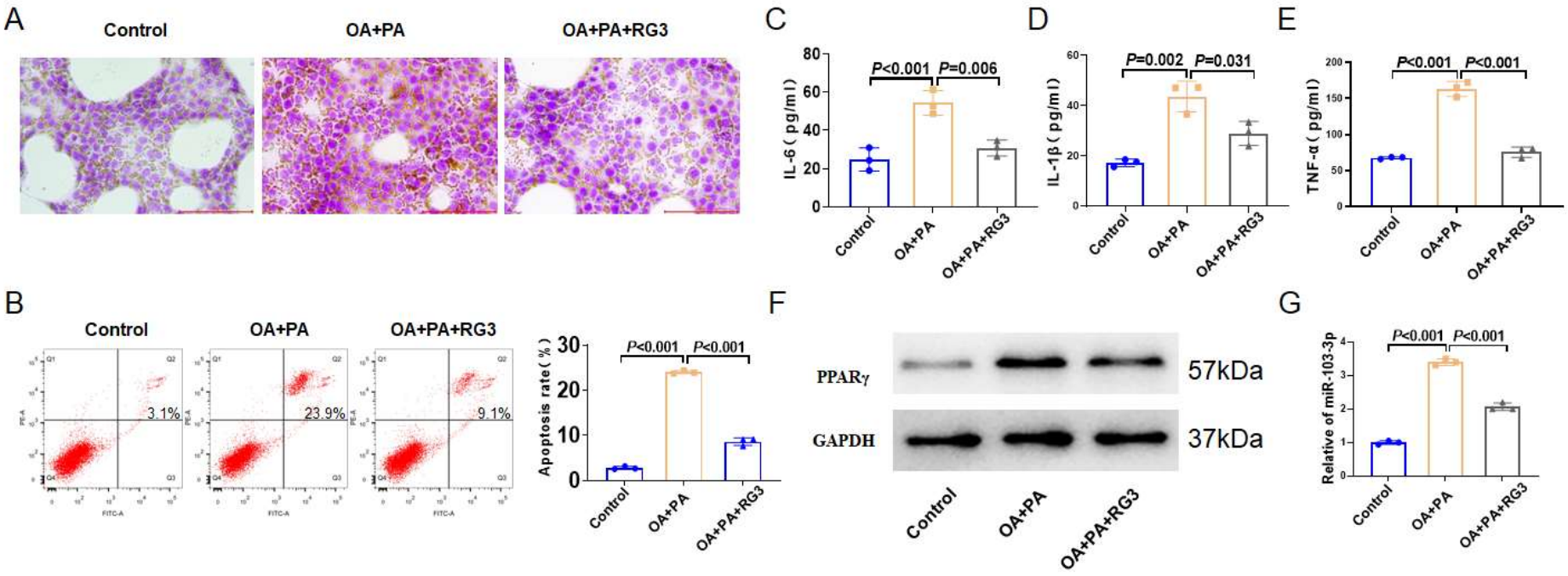

Figure 4: (A)Lipid accumulation in cells; (B) cell apoptosis; (C - E) inflammatory factor levels; (F) PPARγ expression level; (G) miR-103-3p expression level

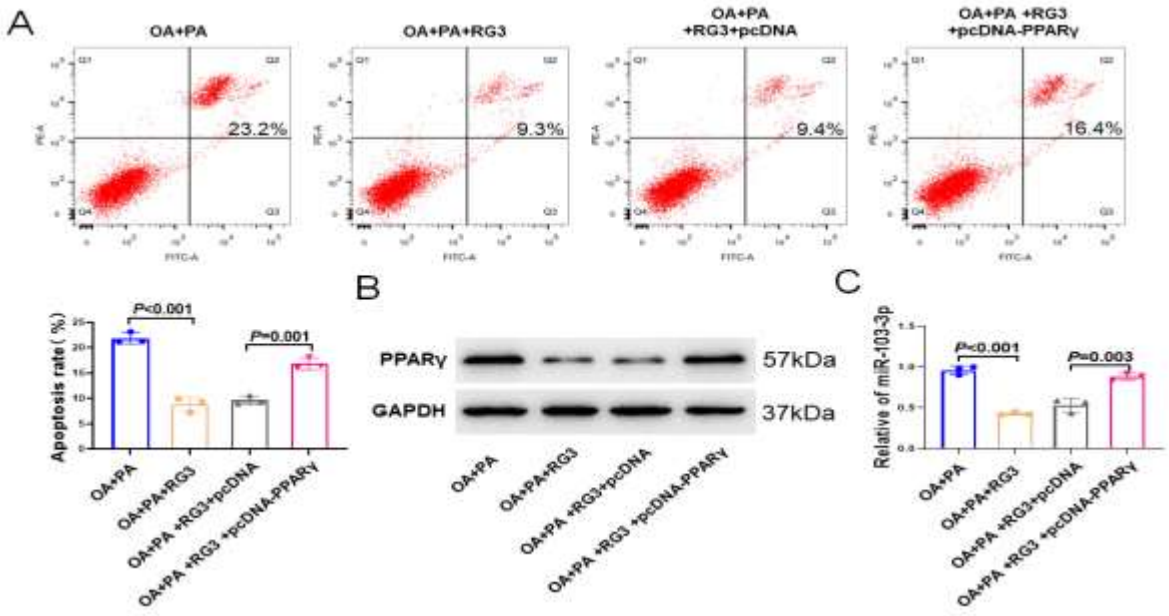

Figure 5: (A) Cell apoptosis; (B) PPARγ expression level; (C) miR-103-3p expression level

DISCUSSION

Research has demonstrated that Rg3 protects the liver through various pharmacological activities. For instance, it exerted anti-hepatic fibrosis effect by inhibiting autophagy flux in acetamide-therapeutic mice and LPS-fueled rat hepatic stellate cells [14]. Moreover, Rg3 has been shown to alleviate hepatocyte injury caused by paracetamol by regulating levels of pro-inflammatory and anti-inflammatory cytokines [15]. Furthermore, Rg3 enhanced ARHGAP9 protein expression and inhibited liver cancer cell migration and invasion. A study demonstrated that Rg3 enhanced autophagy, thereby alleviating sepsis-induced damage to the liver and mitochondria by increasing TUG1 expression and reducing miR-200a-3p expression, resulting in stimulation of the SIRT1/AMPK pathway [16]. The most significant concern in NAFLD is its potential to lead to the slow advancement of liver fibering, interstitial fibrosis and liver cancer and cirrhosis after liver injury [17].

The present study demonstrated that Rg3 significantly inhibited liver cell apoptosis induced by OA and PA, alleviated lipid accumulation, and reduced inflammatory response in liver cells. Moreover, Rg3 showed promising hepatoprotective effects in HFD-induced NAFLD mice. These data indicate that Rg3 has promising efficacy in NAFLD treatment, and its beneficial effects are due to alleviation of liver cell damage.

The findings in the present research are very significant, in that Rg3 exerted a protective effect on liver cells in NAFLD and also produced a regulatory effect on the expression of PPARγ during the treatment of NAFLD. The data obtained revealed that PPARγ was significantly expressed in the liver tissue of HFD-induced NAFLD mice, and also in an *in vitro* mouse liver cell model established with OA and PA. After treatment with Rg3, PPARγ was significantly reduced in the aforementioned mice and liver cells.

Friedman SL *et al* [18] studied the mechanism underlying the use of fermented Korean ginseng extract rich in Rg3 and other ginsenosides, for NAFLD treatment. It was found that it affects the progression of NAFLD by regulating PPARγ, which tallies with findings in the present study. This research has clearly shown that Rg3 inhibited hepatocyte apoptosis in NAFLD through PPARγ, thereby alleviating the progression of NAFLD.

In the animal studies, significant changes in the expression of miR-103-3p in the liver of NAFLD mice treated with Rg3 were found. In previous studies, it was reported that PPARγ was activated by binding to ligands, leading to formation of heterodimers with retinol X-receptor (RXR). Following this, PPARs became bound to PPAR response elements (PPREs) upstream of the target gene promoter, and both regulated its transcription [19]. Genome-wide data set screening showed that PPARγ had binding sites with about 140 miRNAs, and it targeted the regulation of Pank3 and Ppargc1b genes and

their corresponding introns, miR-205 and miR-378, thereby regulating apoptosis and endoplasmic reticulum stress response [20]. To further understand the regulatory effect of Rg3 on PPARγ, the expression of PPARγ in primary hepatocyte models cultured *in vitro* was interfered with. Based on this, it was found that PPARγ and miR-103-3p were down-regulated after treatment with Rg3, but the expression of miR-103-3p was also significantly increased after the overexpression of PPARγ. Thus, PPARγ induced the expression of miR-103-3p. Therefore, in NAFLD, Rg3 protected hepatocytes through the PPARγ/miR-103-3p pathway, and reduced apoptosis and the degree of lipid accumulation in liver cells.

CONCLUSION

The results of the present research have demonstrated that Rg3 exerts a therapeutic effect on NAFLD through the PPARγ/miR-103-3p pathway. Thus, Rg3 is a potential drug candidate for the development of a treatment strategy for NAFLD.

DECLARATIONS

Acknowledgements

This study was financially supported by The Medical and Health Science and Technology Program of Zhejiang Province (no. 2020KY002).

Funding

None provided.

Ethical approval

None provided.

Availability of data and materials

The datasets used and/or analyzed during the current study are available from the corresponding author on reasonable request.

Conflict of Interest

No conflict of interest associated with this work.

Contribution of Authors

The authors declare that this work was done by the authors named in this article and all liabilities pertaining to claims relating to the content of this article will be borne by them.

REFERENCES

1. *Gao H, Zhou L, Zhong Y, Ding Z, Lin S, Hou X, Zhou X, Shao J, Yang F, Zou X, et al. Kindlin-2 haploinsufficiency protects against fatty liver by targeting Foxo1 in mice. Nat Commun. 2022; 13: 1025.*
2. *Luukkonen PK, Qadri S, Ahlholm N, Porthan K, Mannisto V, Sammalkorpi H, Penttila AK, Hakkarainen A, Lehtimaki TE, Gaggini M, et al. Distinct contributions of metabolic dysfunction and genetic risk factors in the pathogenesis of non-alcoholic fatty liver disease. J Hepatol. 2022; 76: 526-535.*
3. *Nassir F. NAFLD: Mechanisms, Treatments, and Biomarkers. Biomolecules. 2022; 12: 824-856.*
4. *Kuang J, J Wang, Y Li, M Li, M Zhao, K Ge, D Zheng, KCP Cheung, B Liao, S Wang, T Chen, Y Zhang, C Wang, G Ji, P Chen, H Zhou, C Xie, A Zhao, W Jia, X Zheng and W Jia. Hyodeoxycholic acid alleviates non-alcoholic fatty liver disease through modulating the gut-liver axis. Cell Metab, 2023. 35: 1752-1766.*
5. *Neuschwander-Tetri, B.A., Therapeutic Landscape for NAFLD in 2020. Gastroenterology, 2020; 158: 1984-1998.*
6. *Zhang GYY, Feng X. Effect of diosmetin on young rats with high-fat diet-induced non-alcoholic fatty liver disease. Trop J Pharm Res. 2021; 20: 315-320.*
7. *Chang GR, Lin WL, Lin TC, Liao HJ, Lu YW. The Ameliorative Effects of Saikosaponin in Thioacetamide-Induced Liver Injury and Non-Alcoholic Fatty Liver Disease in Mice. Int J Mol Sci. 2021; 22.*
8. *Yan LS, Zhang SF, Luo G, Cheng BC, Zhang C, Wang YW, Qiu XY, Zhou XH, Wang QG, Song XL, et al. Schisandrin B mitigates hepatic steatosis and promotes fatty acid oxidation by inducing autophagy through AMPK/mTOR signaling pathway. Metabolism. 2022; 131: 155200.*
9. *Lee JB, Yoon SJ, Lee SH, Lee MS, Jung H, Kim TD, Yoon SR, Choi I, Kim IS, Chung SW, et al. Ginsenoside Rg3 ameliorated HFD-induced hepatic steatosis through downregulation of STAT5-PPARgamma. J Endocrinol. 2017; 235: 223-235.*
10. *Leahy JL. Thiazolidinediones in prediabetes and early type 2 diabetes: what can be learned about that disease's pathogenesis. Curr Diab Rep. 2009; 9: 215-220.*

11. Baumann A, Burger K, Brandt A, Staltner R, Jung F, Rajcic D, Lorenzo Pisarello MJ, Bergheim I. GW9662, a peroxisome proliferator-activated receptor gamma antagonist, attenuates the development of non-alcoholic fatty liver disease. Metabolism. 2022; 133: 155233.
12. Borsting E, Cheng VP, Glass CK, Vallon V, Cunard R. Peroxisome proliferator-activated receptor-gamma agonists repress epithelial sodium channel expression in the kidney. Am J Physiol Renal Physiol. 2012; 302: F540-551.
13. John E, Wienecke-Baldacchino A, Liivrand M, Heinaniemi M, Carlberg C, Sinkkonen L. Dataset integration identifies transcriptional regulation of microRNA genes by PPARgamma in differentiating mouse 3T3-L1 adipocytes. Nucleic Acids Res. 2012; 40: 4446-4460.
14. Ding J, Xia C, Cen P, Li S, Yu L, Zhu J, Jin J. MiR-103-3p promotes hepatic steatosis to aggravate nonalcoholic fatty liver disease by targeting of ACOX1. Mol Biol Rep. 2022; 49: 7297-7305.
15. Liu X, Mi X, Wang Z, Zhang M, Hou J, Jiang S, Wang Y, Chen C, Li W. Ginsenoside Rg3 promotes regression from hepatic fibrosis through reducing inflammation-mediated autophagy signaling pathway. Cell Death Dis. 2020; 11: 454.
16. Gao Y, Yan J, Li J, Li X, Yang S, Chen N, Li L, Zhang L. Ginsenoside Rg3 ameliorates acetaminophen-induced hepatotoxicity by suppressing inflammation and oxidative stress. J Pharm Pharmacol. 2021; 73: 322-331.
17. Wu P, Yu X, Peng Y, Wang QL, Deng LT, Xing W. Ginsenoside Rg3 alleviates septic liver injury by regulating the lncRNA TUG1/miR-200c-3p/SIRT1 axis. J Inflamm (Lond). 2021; 18: 31.
18. Friedman SL, Neuschwander-Tetri BA, Rinella M, Sanyal AJ. Mechanisms of NAFLD development and therapeutic strategies. Nat Med. 2018; 24: 908-922.
19. Choi SY, Park JS, Shon CH, Lee CY, Ryu JM, Son DJ, Hwang BY, Yoo HS, Cho YC, Lee J and others. Fermented Korean Red Ginseng Extract Enriched in Rd and Rg3 Protects against Non-Alcoholic Fatty Liver Disease through Regulation of mTORC1. Nutrients. 2019; 11: 2963.
20. Brust R, Shang J, Fuhrmann J, Mosure SA, Bass J, Cano A, Heidari Z, Chrisman IM, Nemetchek MD, Blayo AL, et al. A structural mechanism for directing corepressor-selective inverse agonism of PPARgamma. Nat Commun. 2018; 9: 4687.
21. Li Y, Jiang J, Liu W, Wang H, Zhao L, Liu S, Li P, Zhang S, Sun C, Wu Y, et al. microRNA-378 promotes autophagy and inhibits apoptosis in skeletal muscle. Proc Natl Acad Sci U S A. 2018; 115: E10849-E10858.